KAWASAKI STEEL TECHNICAL REPORT No. 48 March 2003

Improvement of Motor Performance by Use of High-Efficiency Electrical Steels*



Masayoshi Ishida
Dr. Sci.,
Senior Researcher,
Electrical Steel Lab.,
Technical Res. Labs.

Nobuo Shiga
Senior Researcher,
Electrical Steel Lab.,
Technical Res. Labs.

Kenichi Sadahiro
Senior Researcher,
Electrical Steel Lab.,
Technical Res. Labs.

Synopsis:

The influence of the properties of core materials on the performance of a brushless DC motor and an induction motor, which are representative types often used as drive motors for electric and hybrid vehicles. The efficiency of the brushless DC motor of concentrated winding type can be estimated by the core material iron loss at 400 Hz. By using low-core-loss high-flux-density electrical steels RMHE for this brushless DC motor, efficiencies higher than conventional materials by 0.5–1.0% were obtained with equivalent torque constants. In the three-phase induction motor, high efficiencies were obtained by using RMA having higher magnetic flux densities. The difference between materials in the distribution of local magnetic field strength, magnetic flux density and core loss in motor cores were clarified by local magnetic properties measurement using a contact probe method.

1 Introduction

Electrical steels increasingly occupy an important position in the automobile industry. They are used as core material of automobile parts such as motors, actuators and transformers. In the production lines, they are also used in various industrial motors including servo motors for robots and drive systems.

From the standpoint of energy savings, resource savings and preservation of the global environment,[1,2] various types of electric and hybrid electric vehicles have been developed and put to commercial production, and the number of these vehicles has been increasing rapidly.[3,4]

Recent years have seen increasingly tougher requirements for higher performance and energy savings in various types of motors including high-efficiency motors,[5] as well as requirements for non-oriented electrical steels that are the core materials of these motors, and great progress has recently been made in this respect.[6–8] To further improve motor performance, selection of core materials and material design suited to the features of each type of motor, and optimization techniques for using materials will become increasingly important.

This paper describes techniques for evaluating electrical steels using model motors that can ensure optimum application of electrical steel sheets and improve the efficiency of high-efficiency motors including drive motors of electric and hybrid electric vehicles.

2 Evaluation of Electrical Steels by Model Motors

The influenced of core materials on the efficiency of induction motors has previously been investigated using a single-phase induction motor driven by sinusoidal-wave voltage[9] and an inverter-drive three-phase induction motor.[10] For the two types of motors the optimum material conditions such as Si content to obtain highest efficiency strongly depend on design conditions such as rotation speed and flux density. The optimum properties required of core materials are different in a brushless DC motor, on the other hand, because a brushless DC motor undergoes much less copper loss than an induction motor of the same size.[11]

A further investigation was conducted into the characteristics of brushless DC and induction motors and the relationship between motor performance and the magnetic properties of materials such as iron loss and magnetic flux density using recently developed high efficiency electrical steels.

Stator cores of each model motor were fabricated

* Originally published in *Kawasaki Steel Giho*, **34**(2002)2, 90–95

Table 1 Magnetic properties of used stator core materials

Material	$W_{15/50}$ (W/kg)	B_{50} (T)
35RMHE250	2.07	1.71
35RMHE300	2.38	1.73
50RMHE300	2.40	1.71
50RMHE350	2.64	1.73
35RMA250	2.36	1.72
50RMA350	3.17	1.76
35RM300	2.39	1.68
50RM230	2.16	1.67
50RM400	2.86	1.71
50RM1300	5.16	1.77

Tests made on 25 cm Epstein samples (L + C) after stress relief annealed at 750°C for 2 h in N_2

Table 2 Specifications of tested brushless DC motor

Motor type	Surface permanent magnet type brushless DC motor
Rated power	300 W
Input voltage	48 Vdc
Stator dimensions	ϕ178 (OD) × ϕ75 (ID) × 23 (H) mm
Number of slots	12
Rotor dimensions	ϕ74 (OD) × 23 (H) mm
Number of poles	8
Winding	3-phase star connection, 4 coils/phase

using various kinds of non-oriented electrical steels.[12)]

As materials for stator cores, the JIS standard electrical steel sheet RM,[13)] low-iron-loss, high-flux-density electrical steel sheet after stress-relief annealing RMA,[14)] and low-iron-loss, high-flux-density electrical steel sheet RMHE[15)] were used. **Table 1** shows the iron loss at 1.5 T, 50 Hz $W_{15/50}$ and magnetic flux density at 5 000 A/m B_{50} of each sample after stress-relief annealing. Measurement was carried out in according with JIS[16)] using Epstein test specimens sheared in the rolling direction and in the direction transverse to the rolling direction.

For each type of motor, the size and shape of the stators were fixed and the same rotor was used.

The specifications of the brushless DC motor and its drive circuit system used in the test are shown in **Table 2**. The rated power output was 300 W and the rotor was of a surface-mount permanent magnet type using a rare-earth alloy magnet with 8 poles. After adjusting the drive voltage of the test motor by PWM pulse width and setting it at a predetermined no-load rotational speed, a torque was applied with a load motor and the motor characteristics were measured by the sweep of rotational speed.

Table 3 shows the specifications of the inverter-drive three-phase induction motor with a rated power output of 400 W used for the test. The PWM waveform was generated with a carrier wave of a frequency 40 times as high as the synchronizing frequency. After setting at a

Table 3 Specifications of tested induction motor

Motor type	Inverter-driven induction motor
Rated power	400 W
Rated input voltage	120 V
Stator dimensions	ϕ140 (OD) × ϕ84 (ID) × 66 (H) mm
Number of slots	36
Rotor dimensions	ϕ83 (OD) × 66 (H) mm
Number of poles	6
Winding	3-phase star connection

predetermined no-load rotational speed, the motor characteristics were measured by the sweep of rotational speed by applying a torque.

The measured motor characteristics, which included motor efficiency, torque-rotational speed characteristics, etc. were than subjected to loss analysis.[17)]

3 Evaluation of Electrical Steels in Brushless DC Motor

3.1 Effect of Properties of Electrical Steels on Motor Characteristics

Figure 1 shows the relationship between the maximum value of motor efficiency measured in the sweep process for increasing the torque from the state at a no-load rotational speed of 2 000 rpm and the iron loss $W_{10/400}$ at 1.0 T, 400 Hz (measured in ring samples). This figure also shows measurement data obtained for unannealed materials. The maximum motor efficiency is almost completely determined by the iron loss $W_{10/400}$, and not by the magnetic flux density B_{50} of a core material regardless of whether stress-relief annealing has been performed.

This relationship can be well expressed by the following empirical formula:[18)]

$$\eta = 83.19 + 266.3 / (W + 15.8) \quad \cdots\cdots\cdots\cdots (1)$$

where η denotes the maximum efficiency (%) and W the iron loss of a material $W_{10/400}$ (W/kg).

The rotational speed giving the maximum efficiency

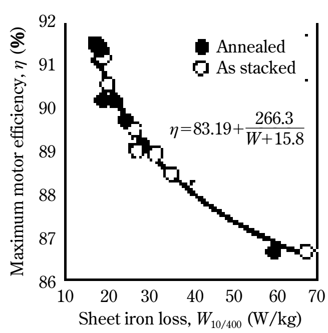

Fig. 1 Relation between sheet iron loss $W_{10/400}$ and maximum motor efficiency of a brushless DC motor

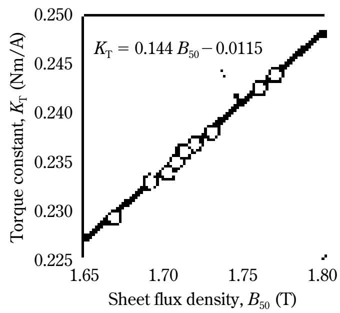

Fig. 2 Relation between sheet flux density B_{50} and torque constant of a brushless DC motor

is in a range from 1 300 to 1 500 rpm and the synchronizing frequency corresponding to this rotational speed range is around 100 Hz. Thus the motor efficiency is determined by an iron loss at relatively high frequency. The effect of higher harmonics in the magnetic flux density generated in the interior of the core is considered to be responsible for this phenomenon that motor efficiency is thus governed by the iron loss at a higher frequency such as 400 Hz.[19)]

In **Fig. 2** the torque constant determined from the torque-current curve is plotted against B_{50} for several materials. The higher the B_{50} value is, the higher the torque constant tends to be.

The relationship between torque constant and B_{50} of a material is expressed satisfactorily by the following linear expression:

$$K_T = 0.144\,B - 0.011\,5 \cdots\cdots\cdots\cdots\cdots\cdots (2)$$

where K_T denotes the torque constant (Nm/A) and B the magnetic flux density of a material B_{50} (T).

The effect of the magnetic flux density of a material on the torque characteristics is clear as shown above. The magnetic flux density of a material, however, has little influence on motor efficiency.

The relationship between the maximum motor efficiency and the torque constant is shown in **Fig. 3**. In this figure, only data on cores after annealing are shown and RMHE and other materials were separately plotted. It is apparent that in terms of torque constants of the same

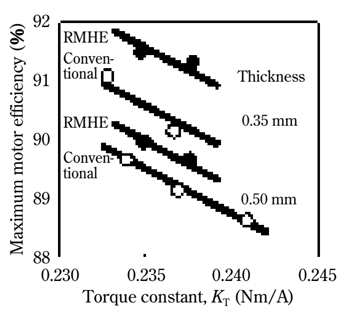

Fig. 3 Relation between torque constant and maximum motor efficiency

level, RMHE shows higher motor efficiency than other materials. This improvement in efficiency by using RMHE depends on sheet thickness: it is about 0.5% (difference in efficiency percentage) at a sheet thickness of 0.50 mm, whereas it is almost 1% at a sheet thickness of 0.35 mm. In terms of values of torque constant for the same efficiency, RMHE shows higher values: they are about 3% (incremental ratio to conventional materials) larger than conventional materials at a sheet thickness of 0.35 mm and about 1.5% larger at a sheet thickness of 0.50 mm. From these results, it is concluded that motor efficiency and torque characteristics can be simultaneously improved by using RMHE.

3.2 Comparison of Electrical Steels by Efficiency Map

The conditions under which motors are used, such as rotational speed, torque, power output, are diverse and even with the same motor, they substantially change depending on the operating conditions. Therefore, in order to select materials suited to practical conditions, it is desirable to express motor characteristics in the form of maps in which drive conditions are employed as variables. Features of various types of electrical steels used in motor cores will be described below using maps in which rotational speed and torque are used as variables.

Figure 4 shows efficiency maps of brushless DC motors in which five types of materials are used as their cores (all cores are annealed). It is apparent that in comparison with the general-purpose material 50RM1300 (e), motor efficiency is improved in the whole mapping range by reducing the iron loss of the material as in 50RM400(d) and 50RM230(c) in this order. In 35RMA250(b), it is noted that the range of high efficiency widens at higher torques. In 35RMHE250(a), the range of high efficiency widens further to the whole area and the efficiency is the highest in all torque-rotational speed ranges. Therefore, it is suggested that 35RMHE250 is most suited to drive motors for automobiles that operate at a high torque and a high speed.

3.3 Comparison of Electrical Steels by Iron Loss and Copper Loss Maps

Loss analysis is important, because the motor efficiency at a constant power output is expressed by:

$$\text{(Motor Efficiency)} = \text{(Power Output)} / \{\text{(Power Output)} + \text{(Loss)}\} \cdots (3)$$

Losses in a motor are classified into copper loss, iron loss, mechanical loss, stray load loss, etc. However, due to practical difficulties to separate the iron loss, mechanical loss and stray load loss from the experimental data, the remainder, which is obtained by deducting the copper loss from the observed total loss, is regarded in the present analysis as the iron loss in the broader sense of the term. It has been ascertained that the mechanical loss in no-load rotation is less than iron loss in the range

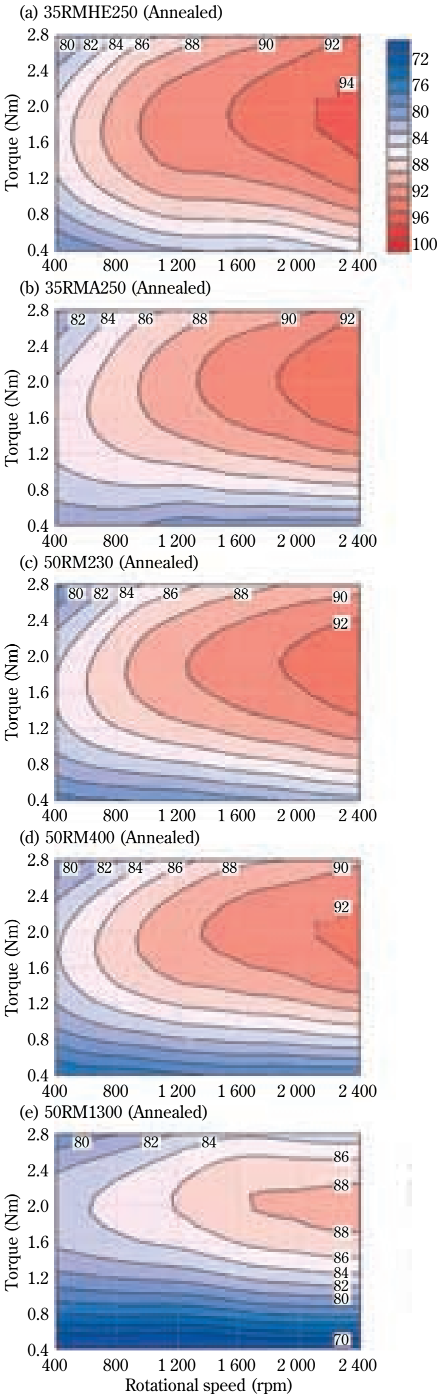

Fig. 4 Efficiency maps of brushless DC motors using (a) 35RMHE250, (b) 35RMA250, (c) 50RM230, (d) 50RM400, and (e) 50RM1300 (all annealed) as core material

shown in the table.

As an example, **Fig. 5** shows a map of total loss of a brushless DC motor using 50RM400 (the core is annealed) in a rotational speed-torque plane. The loss increases as rotational speed and torque increase.

Figure 6 shows the results of copper and iron losses

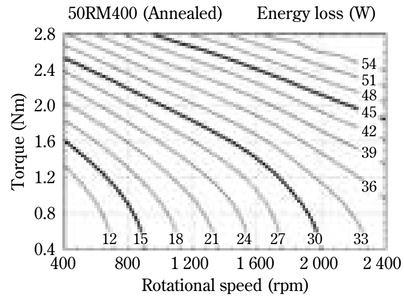

Fig. 5 Energy loss map of a brushless DC motor using 50RM400 as core material

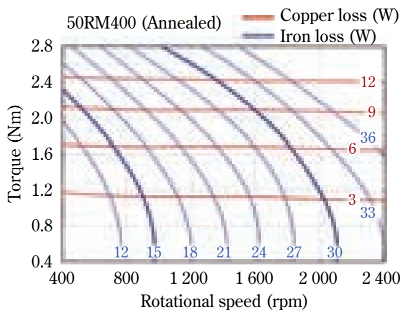

Fig. 6 Copper loss and iron loss map of a brushless DC motor using 50RM400 as core material

calculated from the observed data for the same motor. In the range shown in the figure, the copper loss is almost independent of rotational speed and increases with increasing torque. On the other hand, the iron loss increases with increasing rotational speed, but at the same time increases with increasing torque. Iron loss shows larger values than copper loss with the exception of part of the range of low speed and high torque.

A comparison between Figs. 5 and 6 suggests that the dependence of the loss on rotational speed and torque strongly reflects the behavior of the iron loss (including mechanical loss and stray load loss) which has a predominant effect over the total loss and consequently the motor efficiency.

The tendency of the iron loss to increase with increasing torque is considered to be affected by an increase in the higher harmonic components in magnetic flux density, which occurs simultaneously with increasing armature current, as a result of an increase in torque.[20]

In order to clarify the effect of sheet thickness on motor efficiency, **Fig. 7** shows a comparison of efficiency maps of motors using 35RMHE300 (0.35 mm thick sheet) and 50RMHE300 (0.50 mm thick sheet), both annealed, which have almost the same value of $W_{15/50}$. Although there is no great difference between the two motors in low-speed rotation, the efficiency for the thinner material, 35RMHE300, tends to increase with increasing rotational speed. Also, 35RMHE300 shows a higher efficiency at low torque.

Figure 8 shows maps of iron loss (including mechan-

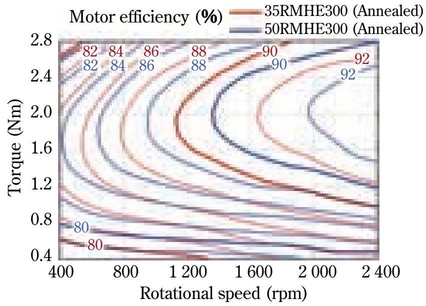

Fig. 7 Efficiency maps of brushless DC motors using 35RMHE300 and 50RMHE300

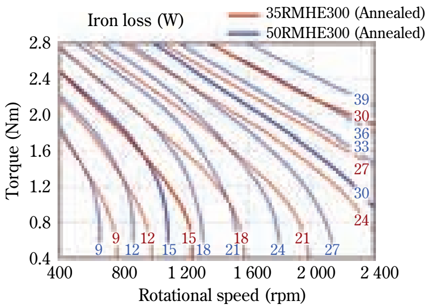

Fig. 8 Iron loss maps of brushless DC motors using 35RMHE300 and 50RMA300 as core material

ical loss and stray load loss) of motor cores of the same 35RMHE300 and 50RMHE300 (both annealed) as shown in the above described efficiency maps. Although the two motor cores show the same degree of motor iron loss at low rotational speeds of about 1 200 rpm or below, 35RMHE300, having a smaller sheet thickness, shows less iron loss than 50RMHE300 with increasing rotational speed. This fact coincides with the feature of thinner material that the increase in iron loss with increasing frequency is less than thicker material. This feature is more significant in an increased rotation speed range. In this manner, the behavior of the efficiency of brushless DC motors of which results are shown in Fig. 7 can be interpreted satisfactorily in terms of the iron loss maps.

4 Evaluation of Electrical Steels in Induction Motors

4.1 Effect of Core Material Properties on Motor Efficiency

Figure 9 shows the maximum efficiency of induction motors, in which various types of electrical steels are used as core material, as a function of material iron loss $W_{15/50}$. This figure shows values for annealed cores. In terms of materials, the maximum motor efficiency tends to increase with decreasing iron loss. However, this dependence is comparatively small and the efficiency

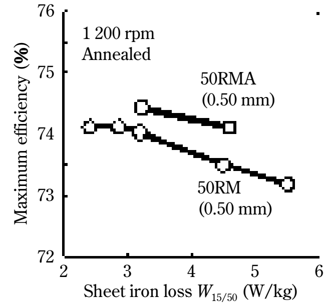

Fig. 9 Relation between maximum motor efficiency of an inverter-drive induction motor and sheet iron loss $W_{15/50}$

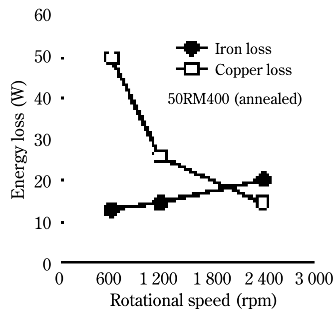

Fig. 10 Copper and iron losses in an inverter-drive induction motor using 50RM400

tends to approach a saturation even in the case of using materials with iron losses less than a certain level. On the other hand, RMA, which is a material having higher flux density B_{50} than the JIS standard material RM with an equivalent iron loss value, clearly shows higher efficiency. This behavior is quite different from that of the brushless DC motor.

In **Fig. 10**, the iron and copper losses of an induction motor consisting of 50RM400 as the core material are shown as a function of rotational speed. The drive conditions are almost the same as those for the maximum efficiency shown in Fig. 9. The range of rotational speed shown in Fig. 10 is almost the same as that of the maps of the characteristics of the brushless DC motors shown in Fig. 4 and following figures. In the range of rotational speed of about 2 000 rpm or less, the copper loss of the motor was greater than its iron loss.

This can be interpreted as follows: In an induction motor secondary copper loss occurs in the rotor of the motor, and therefore, the copper loss fraction increases under the same output power conditions compared with a brushless DC motor of the same size.

Because the iron loss of a motor has a strong correlation with the iron loss of the core material and the copper loss of a motor has a strong correlation with the flux density of the material,[12] this increase in copper loss fraction explains why the maximum efficiency of an induction motor showed a strong dependence on the material flux density B_{50}. Consequently, in induction motors, RMA, having higher B_{50} with the same iron loss $W_{15/50}$, had an advantage in terms of efficiency.

On the other hand, the phenomenon, in which an increase in efficiency tended toward saturation even when a low-iron-loss RM material with $W_{15/50}$ of 3 W/kg or less was used, can be explained as follows: In such a low-iron-loss material, B_{50} decreases because of large amounts of alloying elements and, as a result, copper loss increases.

4.2 Effect of Reduced Iron Loss on Motor Efficiency

As described earlier, a trade-off between the iron loss and copper loss of a motor occurs when the iron loss is reduced by the addition of alloying elements. However, iron loss can be improved without degrading material flux density B_{50}, by reducing the thickness of electrical steel sheet. The dependence of motor efficiency on sheet thickness is shown in **Fig. 11**. It is apparent that in this case, efficiency can be increased with decreasing sheet thickness regardless of rotational speed.

Furthermore, iron loss can also be reduced without degrading B_{50}, by stress-relief annealing of motor cores. The effect of this stress-relief annealing on the reduction in iron loss is shown by the efficiency maps in **Fig. 12**. It is apparent that in all rotational speed-power output ranges, motor efficiency is improved after annealing.

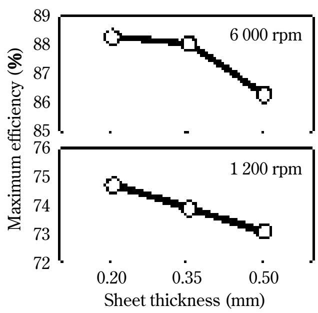

Fig. 11 Maximum efficiency of an inverter-drive induction motor using steels with different thickness

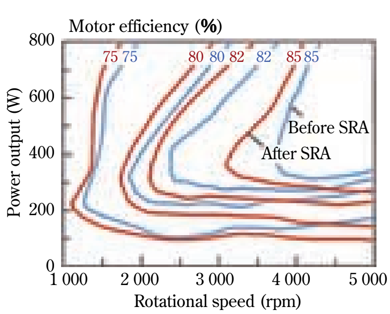

Fig. 12 Comparison of efficiency maps of an inverter-drive induction motor core before and after stress-relief annealing (SRA)

As described above, it became apparent that in an induction motor, an increase in the magnetic flux density of the core material is advantageous for enhancing efficiency, as is a decrease in the iron loss of the core material.

5 Local Magnetic Properties of Induction Motor Core

A local magnetic measurement method based on a contact probe technique[21,22] has been developed for the direct measurement of magnetic properties in a motor core in operation.[23] This method was applied to the local magnetic measurement of the core of a small single-phase induction motor.

A core of a single-phase induction motor of a rated power output of 600 W was used in the measurement. 50RM400 and 50RMA350 were used as the core materials, and annealing and winding were performed after core lamination. At one end of the winding, gaps were provided between the teeth and the winding so that a probe could be inserted immediately above the teeth portion. The magnetic flux density at the end face of the stator core was measured using two pairs of contact probes (in the radial and circumferential directions) and the magnetic field strength near measuring points of magnetic flux density was detected by using a pair of small Hall probes. The measurement was carried out with the motor operated at single phase 60 Hz, 100 V.

The iron loss values at each measuring point were calculated as follows: the area of a hysteresis loop was obtained from the waveforms of the radial and circumferential components of magnetic flux density and magnetic field strength under no-load conditions by Eqs. (4) and (5), and their sum was regarded as a two-dimensional iron loss value W_{2d}:

$$W_{2d} = (f/\rho)\oint \boldsymbol{H}\cdot \mathrm{d}\boldsymbol{B} = W_r + W_\theta \cdots\cdots\cdots (4)$$

$$W_{r\theta} = (f/\rho)\oint \boldsymbol{H}_{r,\theta}\mathrm{d}\boldsymbol{B}_{r,\theta}$$

(The double subscript symbol same order) $\cdots\cdots\cdots (5)$

where f denotes synchronizing frequency and ρ the density of the electrical steel. The closed-loop integral is carried out over a single synchronous period.

Figure 13 shows the distribution of local iron loss in a stator core of a single-phase induction motor using 50RM400 operated at 60 Hz, 100 V under no-load condition. The distribution is such that the local iron loss is large in the teeth portion and small in the yoke portion. The local iron loss also tended to become slightly large along the outer periphery of the slot.

Figure 14 shoes the distribution of differences in the local measurement values (radial components) of magnetic field strength H_m, magnetic flux density B_m and iron loss W when 50RM400 and 50RMA350 are used as core materials. 50RM400 has a larger value of H_m in the

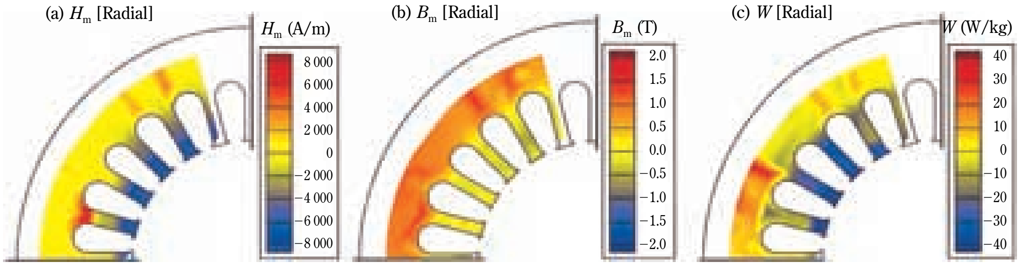

Fig. 14 Difference in distribution of magnetizing force (a), flux density (b) and iron loss (c) between 50RMA and 50RM400 (f [RMA350] $-$ f [RM400])

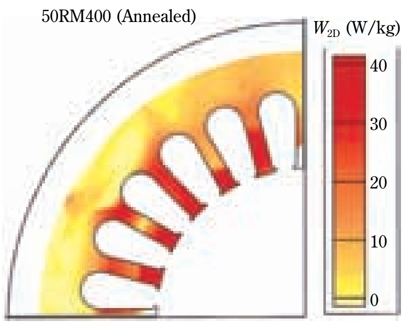

Fig. 13 Distribution of iron loss in stator core using 50RM400 as core material

teeth portion and 50RM400 and 50RMA350 have almost the equal value in the yoke portion. While 50RM400 and 50RMA350 have almost the equal value of B_m in the teeth portion, 50RMA350 has a larger value in the yoke portion. This difference in B_m distribution reflects the fact that 50RMA350 has a higher value of B_{50} than that of 50RM400.

The iron loss distribution reflects the distribution of B_m; 50RM400 shows a larger value in the teeth portion and 50RMA350 shows in places larger values in the yoke portion. As a result, the iron loss of 50RMA350 was less than that of 50RM400 in the whole core.

As described so far, the distribution of iron loss in a core mostly reflects the magnetic flux density distribution determined by the magnetizing characteristics of the core material. This result indicates that an increase of B_{50} of the core material can improve the efficiency of an induction motor. A quantitative interpretation of such measured results would be an interesting subject of future research.

6 Conclusions

An investigation was conducted into the influence of the properties of core materials on the performance, particularly motor efficiency, of a brushless DC motor and an induction motor, which are most frequently used as drive motors for electric and hybrid electric vehicles. The following results were obtained:

(1) Under the rated conditions, the maximum efficiency of a brushless DC motor of the concentrated winding type containing arare-earth alloy magnet can be accurately estimated by the core material iron loss at 400 Hz.

(2) When low-core-loss, high-flux-density electrical steels RMHE are used in the brushless DC motor, efficiency can be improved by 0.5 to 1.0% compared with conventional materials with equivalent torque constants.

(3) In a three-phase induction motor, efficiency can be increased by using RMA as a core material, due to its higher magnetic flux density B_{50}.

(4) Differences between RMA and RM in the distribution of local magnetic field strength, magnetic flux density and core loss in motor cores were clarified by the measurement of local magnetic properties using a contact probe method.

References

1) The Agency of Natural Resources and Energy, Supervision: "Natural Resource and Energy 1999/2000", (1999)
2) Y. Daisho: "A Prospect on Automobiles for the 21st Century—Resolving Problems Associated with Environment and Energy—", *J. Soc. Automot. Eng. Jpn.*, **56**(2002)1, 18
3) IEEJ Investigation Committee on Drive Systems for Electric Vehicles, Ed.: "State-of-the-Art Technology of Electric Vehicles", (1999), [Ohmsha]
4) H. Hirose and S. Tange: "Present Situations and Future Prospects of Electric Vehicles and Hybrid Electric Vehicles", *J. Soc. Automot. Eng. Jpn.*, **56**(2002)1, 36
5) IEEJ Investigation Committee on Improvement of Small Motors, Ed.: "Improvement of Small Motors", Tech. Rep., IEE Jpn., (1999)744
6) M. Ishida: "Recent Progress in Non-Oriented Electrical Steels and Their Properties in Applications", *J. Magn. Soc. Jpn.*, **25**(2001)1, 3
7) A. Honda, K. Senda, and K. Sadahiro: "Electrical Steel for Motors of Electric and Hybrid Vehicles", *Kawasaki Steel Technical Report*, (2003)48, 33
8) M. Kawano, T. Fujiyama, and T. Aoki: "Electrical Steels for High-Functional Automotive Electrical Components Corresponding to Energy Saving", *Kawasaki Steel Technical Report*, (2003)48, 47
9) A. Honda, B. Fukuda, I. Ohyama, and Y. Mine: "Effects of Magnetic Properties of Nonoriented Electrical Steel Sheets on Motor Efficiency", *J. Mater. Eng.*, **12**(1990)1, 141
10) A. Honda, K. Sato, M. Ishida, and I. Ohyama: "Effects of

Core Materials on Properties of AC Induction Motor", Papers of Technical Meeting on Rotating Machinery, IEE Jpn., RM-97-148, (1997)
11) M. Ishida, A. Inenaga, A. Honda, and I. Ohyama: "Influence of Core Material on Performance of Brushless DC Motor", Papers of Technical Meeting on Rotating Machinery, IEE Jpn., RM-98-147, (1998)
12) M. Ishida, N. Shiga, M. Kawano, A. Honda, M. Komatsubara, and I. Ohyama: *J. Jpn. Soc. Appl. Electromagn. and Mech*., **7**(1999)3, 248
13) "RM-CORE, Non Oriented Magnetic Steel Strip", Catalog, Kawasaki Steel
14) M. Takashima, M. Shinohara, A. Honda, S. Okamura, and N. Morito: *Materia Jpn*., **36**(1997)4, 385
15) K. Sakai, M. Kawano, and T. Fujiyama: "Non-Oriented Electrical Steel Having Excellent Punchability for High-Efficiency Motor", *Kawasaki Steel Giho*, **33**(2001)2, 92
16) Japanese Industrial Standard, JIS C 2552, (2000)
17) T. Sawahata, M. Miyagawa, H. Ito, K. Morimoto, and T. Shimazaki: *National Tech. Rep*., **33**(1987)5, 617
18) K. Sadahiro, N. Shiga, and M. Ishida: "Analysis Technology Used in Development of High-Efficiency Electrical Steels and Their Optimized Application to Electrical Apparatuses", *Kawasaki Steel Giho*, **33**(2001)3, 103
19) N. Shiga, M. Ishida, and I. Ohyama: "Operating Flux Density of a Brushless DC Motor Core in Relation to Material Properties", Papers of Technical Meeting on Magnetics, IEE Jpn., MAG-00-269, (2000)
20) M. Ishida, N. Shiga, and K. Sadahiro: "A Simple Model for Influence of Core Material on the Performance of a Brushless DC Motor", Papers of Technical Meeting on Magnetics, IEE Jpn., MAG-01-125, (2001)
21) T. Yamaguchi, M. Imamura, K. Senda, M. Ishida, K. Sato, A. Honda, and T. Yamamoto: "Analytical Evaluation of the Accuracy of Localized Magnetic Flux Measurement by the Stylus Probe Method", *Trans. Inst. Electr. Eng. Jpn*., **115-A**(1995)1, 50
22) K. Senda, M. Ishida, K. Sato, M. Komatsubara, and T. Yamaguchi: "Localized Magnetic Properties in Grain-Oriented Silicon Steel Measured by Stylus Probe Method", *Trans. Inst. Electr. Eng. Jpn*., **117-A**(1997)9, 942
23) M. Ishida, A. Honda, M. Komatsubara, K. Sato, and I. Ohyama: Papers of Technical Meeting on Rotating Machinery, IEE Jpn., RM-99-22, (1999)